Hindawi Publishing Corporation
Journal of Electrical and Computer Engineering
Volume 2013, Article ID 382913, 10 pages
http://dx.doi.org/10.1155/2013/382913

Research Article

A Compact, Versatile Six-Port Radar Module for Industrial and Medical Applications

Sarah Linz,[1] Gabor Vinci,[2] Sebastian Mann,[1] Stefan Lindner,[1] Francesco Barbon,[1] R. Weigel,[1] and Alexander Koelpin[1]

[1] *Institute for Electronics Engineering, University of Erlangen-Nuremberg, 91058 Erlangen, Germany*
[2] *InnoSenT GmbH, Am Roedentor 30, 97499 Donnersdorf, Germany*

Correspondence should be addressed to Sarah Linz; sarah.linz@fau.de

Received 4 October 2013; Accepted 21 November 2013

Academic Editor: Adriana Serban

The Six-port receiver has been intensively investigated in the last decade to be implemented as an alternative radar architecture. Plenty of current scientific publications demonstrate the effectiveness and versatility of the Six-port radar for special industrial, automotive, and medical applications, ranging from accurate contactless vibration analysis, through automotive radar calibration, to remote breath and heartbeat monitoring. Its highlights, such as excellent phase discrimination, trivial signal processing, low circuit complexity, and cost, have lately drawn the attention of companies working with radar technology. A joint project involving the University of Erlangen-Nuremberg and InnoSenT GmbH (Innovative Sensor Technology) led to the development of a highly accurate, compact, and versatile Six-port radar module aiming at a reliable high-integration of all subcomponents such as antenna, Six-port front-end, baseband circuitry, and digital signal processing in one single package. Innovative aspects in the RF front-end design as well as in the integration strategy are hereby presented, together with a system overview and measurement results.

1. Introduction

Optical high-resolution, contactless distance measurement techniques such as laser interferometry and laser pulse time-difference measurements have been widely implemented for industrial and medical applications. The drawback of optical techniques is the difficulty to penetrate dust and fog with the laser in harsh environments as optical lenses and mirrors can get dirty. Furthermore, with increasing suspended particle density in the propagation environment dampening and scattering effects increase so that the laser cannot reach the surface of the object under investigation. These inconveniences of laser based systems are the cause of an increasing interest in alternative nonoptical measurement techniques that are robust against such industrial environment conditions.

One of the main noncontact-based alternatives to laser is radar. Radar-based measurement techniques work also when a direct optical line of sight to the object under investigation is not guaranteed since radar waves can propagate much better through foggy or dusty air. Furthermore, even bulky and optically nontransparent dielectric slabs or nonmetallic shields can be penetrated by the radar signal [1, 2].

Within the last decade, radar technology has been rapidly expanding in industrial, automotive, and medical application areas [3]. Advanced positioning and sensor feedback tasks in automation processes rely on high precision radar-based distance detection, for example, to measure and track the movement of robots [4]. As an example for medical applications, high measurement accuracy is required to guarantee the safety of patients and the quality of therapies through vital sign monitoring systems. For instance, heartbeat and breath rate monitoring is of primary interest and can be achieved with particularly accurate radar-based displacement detection techniques [5].

The Six-port receiver recently raised the interest of the industry [6]. The excellent phase resolution offered by this alternative microwave receiver leads to high accuracy distance and angular measurement capabilities [7]. Historically, the Six-port receiver has been used as a reflectometer [8, 9].

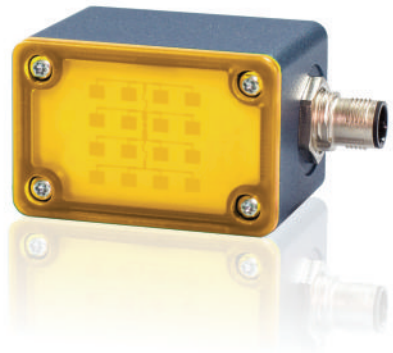

Figure 1: The developed Six-port radar module.

Following the evolution of radar and microwave technology, the Six-port receiver has been also used as an alternative vector network analyzer for sensing applications. Mainly due to the progress in material and process technology, the Six-port technique has lately found several other implementation possibilities. As a result of a joint project involving the University of Erlangen-Nuremberg and InnoSenT GmbH (Innovative Sensor Technology), a radar sensor based on the Six-port technique has been developed (Figure 1).

In this work, this compact and versatile Six-port radar system is presented along with design and simulation results of its passive components as well as hardware measurements and evaluations. The principles of Six-port receivers as well as the use of Six-port networks for radar applications have already been shown in many publications [9–11]. The developed monostatic Six-port radar front-end works in the ISM band at 24 GHz. It can be used in one-target scenarios for distance and vibration measurements [12]. After using a suitable calibration, the position and movement of a target can be calculated [11].

2. System Overview

The presented sensor is a monostatic Six-port radar with integrated patch antenna array, microwave front-end, and digital signal processing (DSP) board in one compact case measuring only $(40 \times 60 \times 44)\,\text{mm}^3$ (width, length, height).

The schematic view of the system concept is shown in Figure 2. The reference signal generated by a fractional-N frequency synthesizer is routed to the input port 1 of the Six-port. The transmit signal is sent to the target by a 16 elements patch array antenna with 14 dBi gain and 40° angular width (3 dB). The reflected signal from the target is coupled to the receive path and therefore fed into port 2 of the Six-port receiver. Its four output signals are downconverted to baseband by four Schottky diode power detectors and amplified with the help of two dual operational amplifiers. The analog-to-digital conversion, error correction, and calculation of the target's position or movement are done using a dedicated DSP board.

Due to the use of a low-noise amplifier (LNA) with 18 dB gain in the receive path and two digitally adjustable attenuators in the reference as well as in the receive path, the system can be adapted to a variety of application scenarios. The attenuators can be programmed via SPI interfaces. The high flexibility of the system is needed because of the free space measurement environment. Depending on the distance between antenna and target as well as the target's dimensions, the received power level may strongly vary.

Like in monostatic multiplicative mixer based radar systems, the isolation of the radar coupler and the matching of the antenna are crucial for the system's performance [13]. Crosstalk from transmit to receive path creates a DC-offset in the baseband voltages. This may shift the operating point of the diode detectors to a nonquadratic region and may drive the operational amplifiers into saturation.

The microwave signal is generated by a fractional-N frequency synthesizer which also allows frequency and phase modulation. The synthesizer has been partly developed by InnoSenT GmbH (VCO, attenuator, and buffer amplifier) and is specified to have an output power of 8 dBm.

3. The Six-Port Receiver Front-End

The Six-port network is an alternative receiver setup for microwave and millimeter-wave frequencies. It is essentially a passive receiver structure based on the interferometric principle featuring two input ports and four output ports [14]. Two input signals are superimposed under four relative quadrature phase shifts. Depending on phase difference and amplitudes of the two input signals, constructive and destructive interaction takes place at the four output ports. Two complex input signals $\underline{P_1}$ and $\underline{P_2}$ (Figure 2) with carrier frequency f are hereby defined as

$$\begin{aligned} \underline{P_1} &= A_1 \cdot e^{j(2\pi f t + \phi_1)}; \\ \underline{P_2} &= A_2 \cdot e^{j(2\pi f t + \phi_2)}. \end{aligned} \tag{1}$$

The complex output signals $\underline{P_3}$, $\underline{P_4}$, $\underline{P_5}$, and $\underline{P_6}$ are therefore generated. Diode-based power detectors (Square-law) at the four outputs of the Six-port receiver deliver four baseband voltages B_3 to B_6 (Figure 2):

$$\begin{aligned} B_3 &= \left|\underline{P_3}\right|^2 = 0.25\left|\underline{P_1} + j\underline{P_2}\right|^2; \\ B_4 &= \left|\underline{P_4}\right|^2 = 0.25\left|j\underline{P_1} + \underline{P_2}\right|^2; \\ B_5 &= \left|\underline{P_5}\right|^2 = 0.25\left|j\underline{P_1} + j\underline{P_2}\right|^2; \\ B_6 &= \left|\underline{P_6}\right|^2 = 0.25\left|\underline{P_1} - \underline{P_2}\right|^2. \end{aligned} \tag{2}$$

Due to the quadrature phase shift superposition of the input signals, a complex quantity $\underline{Z}$ can be defined by the four baseband voltages. Therefore, the baseband signals B_3 to B_6 can be seen as differential I/Q-signals of a complex receiver according to

$$\underline{Z} = I + jQ = \left(B_5 - B_6\right) + j\left(B_3 - B_4\right). \tag{3}$$

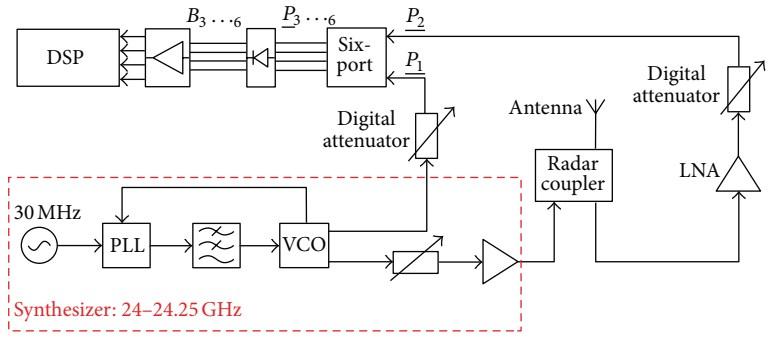

Figure 2: Schematical view of the radar front-end.

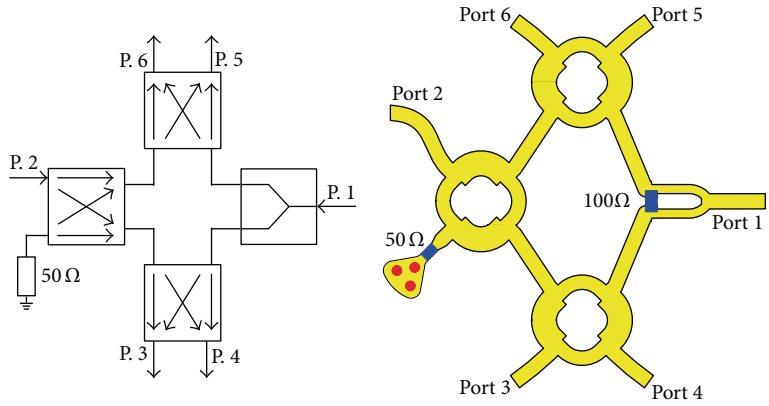

Figure 3: Schematical view and layout of the Six-port network.

Finally, the argument of $\underline{Z}$ can be calculated delivering the phase shift between the two input signals of the Six-port:

$$\Delta\sigma = \phi_1 - \phi_2 = \arg\{\underline{Z}\}. \tag{4}$$

When using the Six-port as a receiver for radar applications, the phase shift $\Delta\sigma$ comprises the distance information and can be directly renormalized when the wavelength of the signal is known [11]:

$$d = \lambda \frac{\Delta\sigma}{2 \cdot 2\pi}. \tag{5}$$

Since the measurement relies on a phase difference evaluation, an ambiguity in the measurement will occur if the distance to be measured is greater than half the wavelength of the radar signal. Nevertheless, as described in Section 4, by using appropriate modulation schemes the ambiguity in phase can be resolved to determine a unique distance measurement to the target.

In Figure 3, the circuit schematic and hardware implementation in microstrip technology of the developed Six-port network can be seen. A Wilkinson power divider and three quadrature hybrid couplers, also called branchline couplers, generate the mentioned phase shifts.

4. Digital Signal Processing

After some analog signal conditioning procedures in baseband, the output signals from the Six-port receiver are sampled by synchronously triggered analog-to-digital converters (ADC) and evaluated by a microcontroller that manages the complete sensor module. The sampling rate is set to 250 kHz and the resolution of the ADCs is 12-bit. The calculated distance information is made available through an RS-232 parallel port in a 32-bit floating point format.

A system initialization is performed directly after start-up to adapt the radar sensor's parameters to the environment. The appropriate reference as well as receive power levels are adjusted following the routine expressed in the flowchart in Figure 4 to compensate for power imbalance. For this purpose, a Frequency Modulated Continuous Wave (FMCW) signal is used. The reference power level is adjusted through a digital, variable attenuator with the $\mathrm{Att}_{\mathrm{ref}}$ value while $\mathrm{Att}_{\mathrm{rx}}$ controls the attenuator in the receive path. Both attenuators can be set to values between 0 and 31 dB. Furthermore, the LNA in the receive path can be completely switched off for calibration and initialization purposes.

To avoid the well-known ambiguity issue of the Six-port receiver, a Frequency Shift Keying (FSK) modulation scheme according to the dual tone approach presented in [15] is implemented. The fractional-N frequency synthesizer generates two tones with a frequency offset of 75 MHz for a maximum nonambiguous range of 2 m. A further FMCW

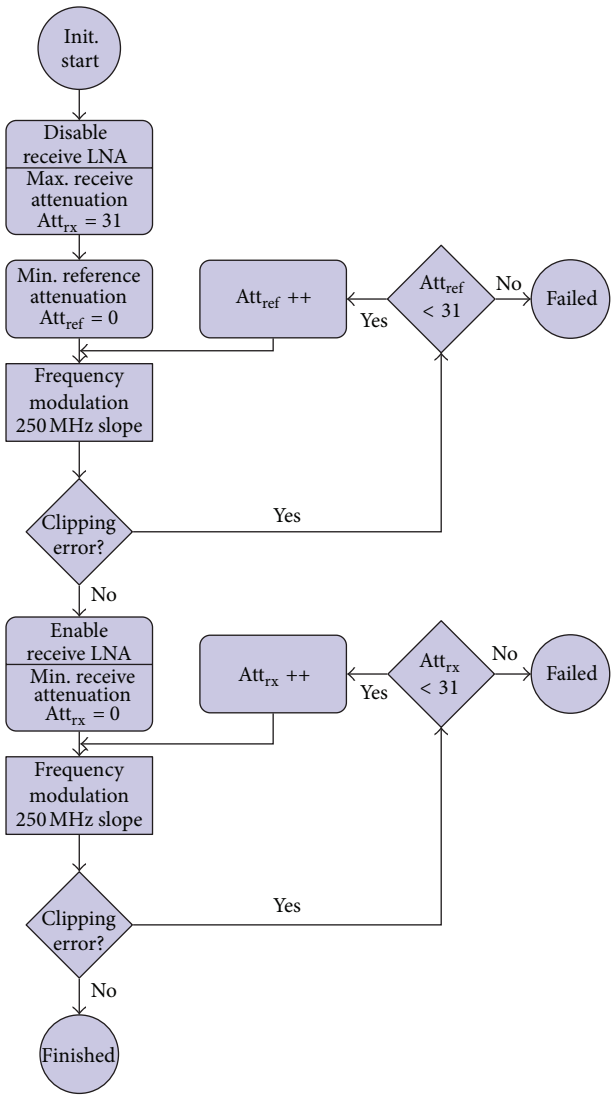

Figure 4: Initialization diagram.

modulation scheme can be implemented to evaluate speed and range of a target, as described in [16].

5. Simulation and Analysis

The simulation results of the passive microwave components are shown in this chapter. The results were obtained with the 3D electromagnetic field simulator CST Microwave Studio using the Frequency Domain Solver. For more details about the theory of the basic circuits (i.e., Wilkinson power divider, quadrature hybrid coupler) the reader may refer to [17] and for the Six-port network to [10].

5.1. Quadrature Hybrid Coupler. The layout for a round quadrature hybrid coupler at 24 GHz is shown in Figure 6(a). The incident wave is fed to port 1, port 4 is isolated, and port 2 and 3 are the output ports. The transmission line length between the ports is a quarter of the wavelength. A round layout has been chosen, because the geometrical 90° angle

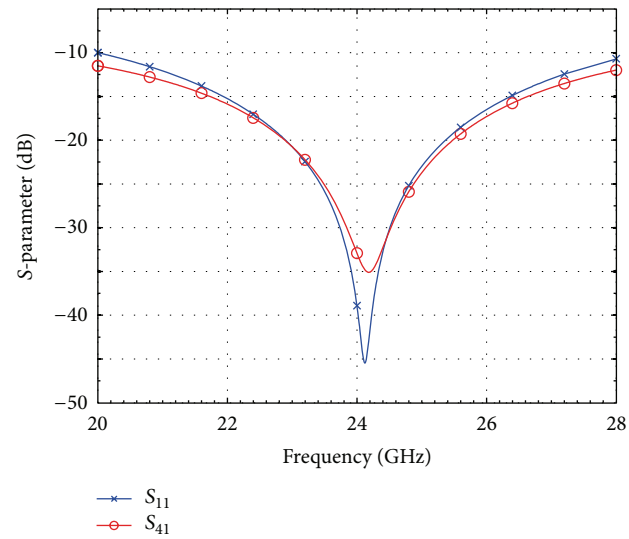

Figure 5: Simulated S_{11} and S_{41} of the quadrature hybrid coupler.

between port 1 and 4 as illustrated in Figure 6(a) leads to a higher isolation, which is a crucial parameter for radar couplers.

Figure 5 shows the simulated input reflection coefficient at port 1 (S_{11} (dB)) and the isolation between port 1 and 4 (S_{41} (dB)). The hybrid coupler is well matched within the entire bandwidth (−38 dB at 24 GHz and 24.25 GHz and −45 dB at the center frequency). The isolation is higher than 33 dB in the frequency band of interest. Due to the high isolation values, the coupler is also used as radar coupler with one port being terminated.

The simulation results for the transmission are presented in Figure 7. For an ideal hybrid coupler the transmission loss would be −3 dB and the phase difference would be 90°. For 24 GHz the required phase difference is reached. However, the transmission loss between port 1 and 3 is −3.2 dB and −3.7 dB between port 1 and 2 although the path length to port 3 is longer than to port 2. A reason for this unexpected difference may be the geometrical 90° angle between port 1 and 2.

5.2. Wilkinson Power Divider. The layout of the Wilkinson power divider is shown in Figure 6(b). It has been optimized to have a good matching at all ports and a high isolation between port 2 and 3 for 24 GHz. According to the simulation results shown in Figure 8, matching of port 1 and 2 as well as transmission between port 2 and 3 are below −20 dB. This is necessary to avoid standing waves inside the Six-port network and coupling between the four Schottky diode power detectors.

5.3. Six-Port Network. In Section 3, it has been demonstrated by (2) that the Six-port receiver relies on four quadrature phase shifts. In the Six-port network used in this work these phase shifts are generated by three branchline couplers and one Wilkinson power divider. The schematic and the layout of the resulting network are presented in Figure 3.

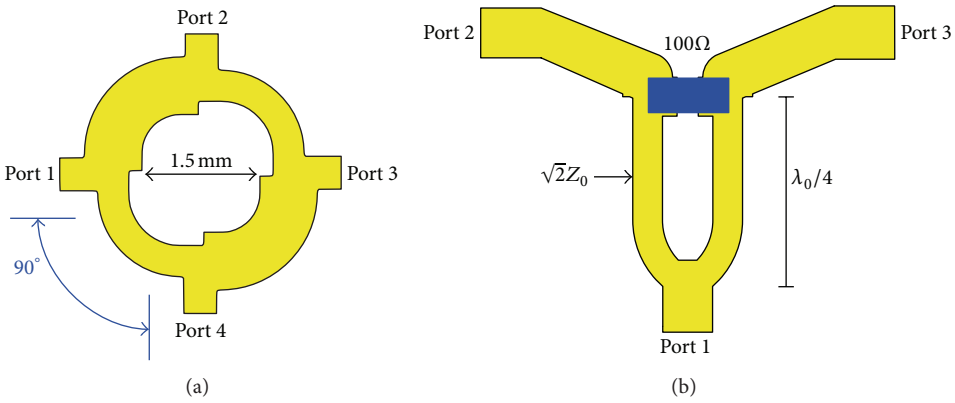

FIGURE 6: Layout of (a) 90° hybrid coupler and (b) Wilkinson power divider.

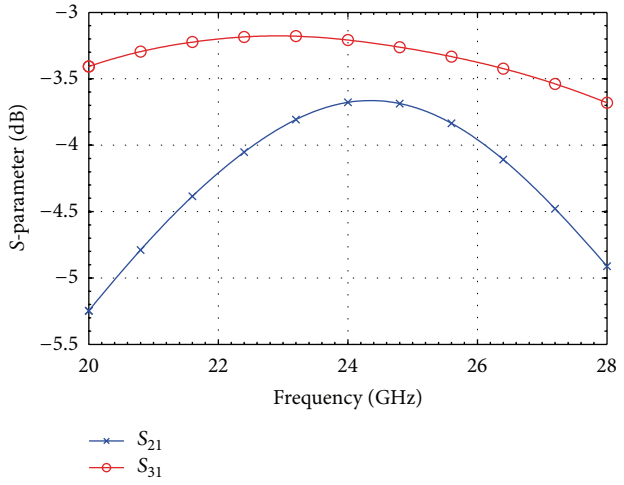

FIGURE 7: Simulated transmission coefficient of coupler.

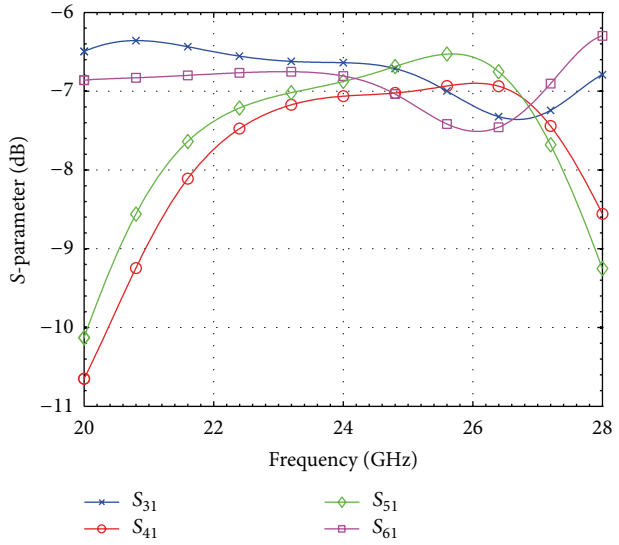

FIGURE 9: Six-port: simulated transmission from port 1 to the output ports.

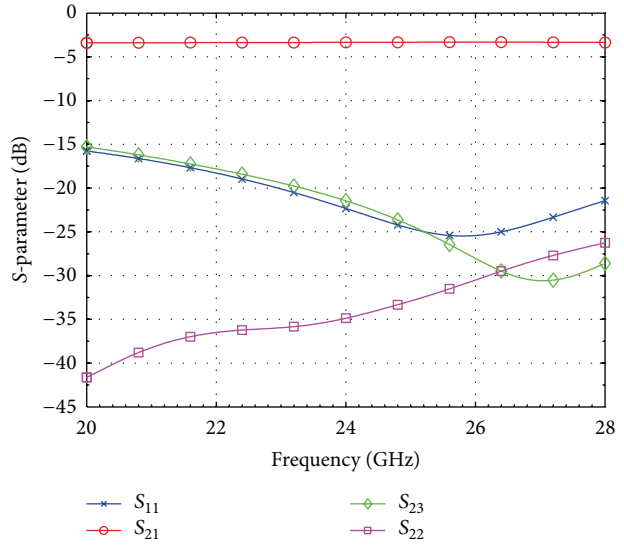

FIGURE 8: Simulated scattering parameters of power divider.

3D field simulation shows that the power imbalance of the transmission from the input to the output ports is less than 2 dB (Figures 9 and 10) and the relative phase shifts match 90° with only 4° error (Figure 11). The reflection coefficient of the input ports and the isolation between them are below −20 dB for 24.125 GHz ± 125 MHz.

6. Applications Overview

6.1. Distance Measurement. High-resolution distance measurements with short and long range positioning are important for a large number of sensing applications [18]. The radar module implements a fractional-N frequency synthesizer enabling different modulation schemes to perform nonambiguous distance measurements. The Six-port receiver suffers from ambiguity issues if distances of more than half a wavelength are measured. A solution to this problem is to use a two or more tone FSK modulation of the carrier

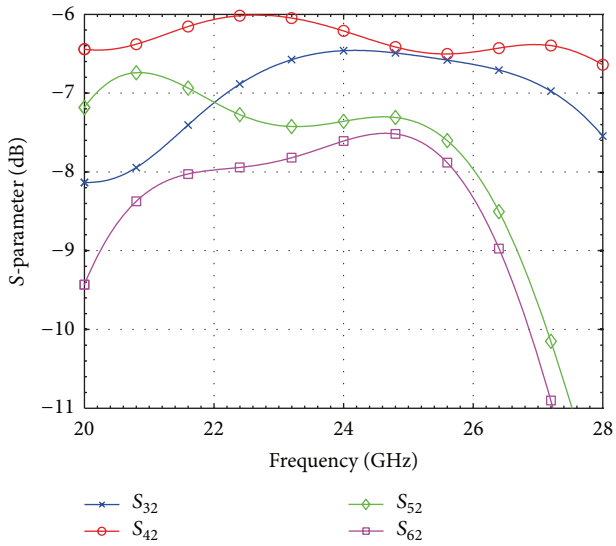

FIGURE 10: Six-port: simulated transmission from port 2 to the output ports.

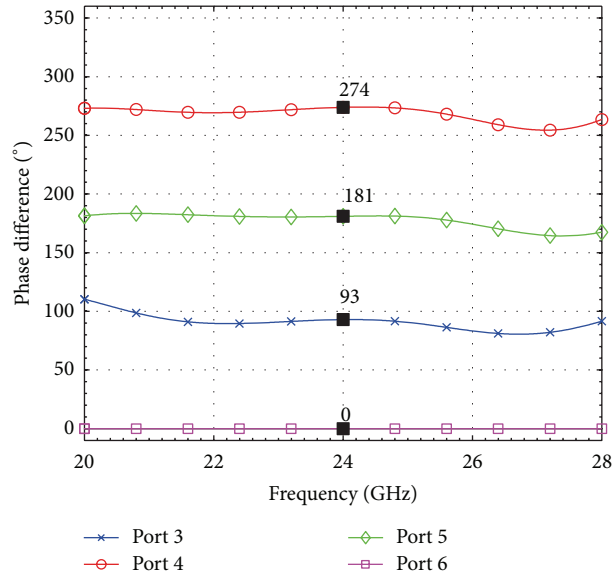

FIGURE 11: Simulated normalized phase difference at the output ports of the Six-port network (reference port 6 is set to 0°).

frequency and comparing the observed phase differences of these signals to each other. This allows to measure distances of several wavelengths with subwavelength accuracy and ultralow tolerances.

6.2. Vibration Measurement. Particularly interesting is the analysis of small displacements of an observed target, for instance, vibration monitoring [2]. Since the Six-port based radar sensor provides very high accuracy distance detection, even the smallest vibrations (i.e., distance variations of the target surface with respect to the sensor) can be accurately detected. Performing a frequency domain analysis, a spectrogram of the target's mechanical vibrations can be obtained. This leads to relevant information about the working conditions of diverse industrial machinery. The sensor can be used for modal analysis in order to measure the dynamic response of mechanical structures and the different vibration modes. By observing for instance a rotating turbine, thus illuminating the complete machine with the Six-port radar, the main mechanical resonances can be recorded and monitored. In case of a mechanical malfunction or degradation, for instance a wearing of the axis bearings, minor changes in the mechanical resonances will occur. Such effects can be therefore monitored without even applying sensors directly to the machine. In other words, a contactless vibration analysis for diverse industrial machines can be easily performed. As the reconstruction algorithms feature low complexity and can be calculated very fast, the maximum detectable vibration frequency is only limited by the sampling frequency of the analog-digital interface.

6.3. Contactless Heartbeat and Respiration Monitoring. For medical applications, the heartbeat and breathing activities affect the phase of the reflected signal which is compared with the reference signal source in the radar device [11]. A radar signal is sent towards the person under test to observe minor mechanical movements of the patient's body. These movements are caused by the respiration as well as heartbeat and can be tracked by analyzing the phase modulation of the backscattered signal. The patients respiration will result in a significant and periodic extension of the torso, which is in the range of several millimeters. Additionally, the heartbeat will be superimposed to this movement, which is assumed to be in the submillimeter range. These periodic movements and vibrations can subsequently be detected by signal postprocessing.

7. Measurements

The passive RF subcomponents have been fabricated on a test PCB based on the Rogers RO4835 substrate material and characterized with a vector network analyzer. The results are shown in Sections 7.1 and 7.2. Furthermore, evaluation measurements of the complete system are presented in Section 7.4. A photo of the RF front-end is shown in Figure 12.

7.1. Quadrature Hybrid Coupler. The properties of the radar coupler are crucial for the performance of the overall system. Therefore, measurement results for this component are hereby presented. As illustrated in Figure 13, the isolation between port 1 and 4 (S_{41} (dB)) of the proposed coupler between 24 and 24.25 GHz is higher than 25 dB, whereas the isolation between port 2 and 3 (S_{32} (dB)) is higher than 30 dB. Since the coupler has been designed to be symmetrical the deviation between S_{41} and S_{32} results from fabrication and measurement inaccuracies. The power imbalance in the transmission from port 1 to ports 2 and 3 is 0.2 dB only (Figure 14). The generated phase difference between ports 2 and 3 varies between 88.1° and 87.3°, which leads to the four quadrature phase shifts of the Six-port network. The ideal phase shift is 90°.

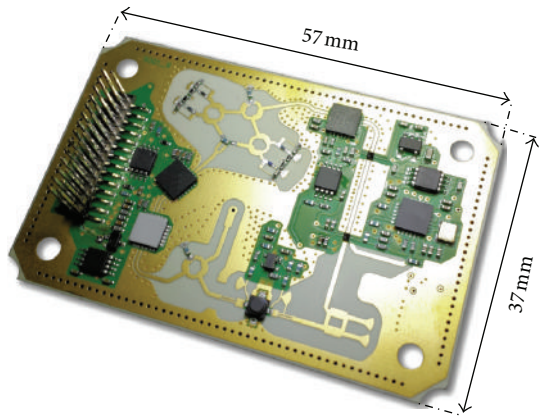

Figure 12: Photo of the radar front-end.

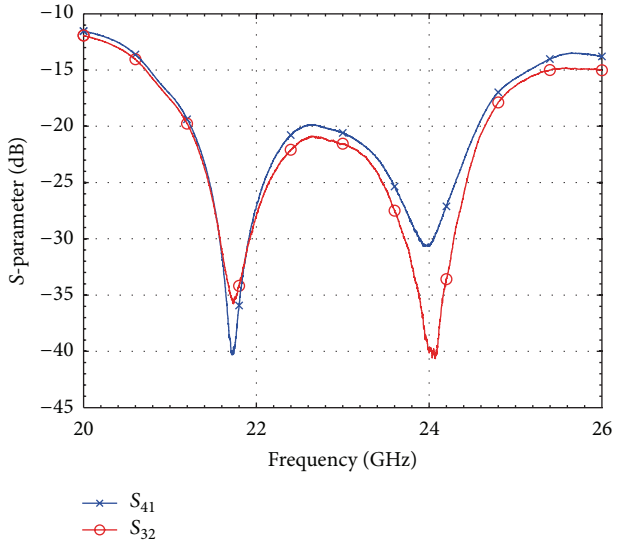

Figure 13: Measured S_{41} and S_{32} of the hybrid coupler.

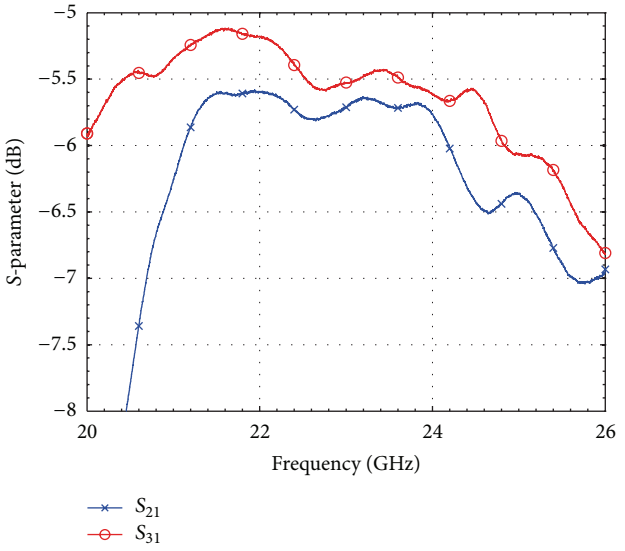

Figure 14: Measured transmission coefficient of the hybrid coupler.

Table 1: Normalized phase difference at the output ports.

Frequency	24 GHz	24.25 GHz	Ideal
Port 3	92.2°	91.3°	90°
Port 4	272.1°	270.9°	270°
Port 5	181.3°	179.5°	180°

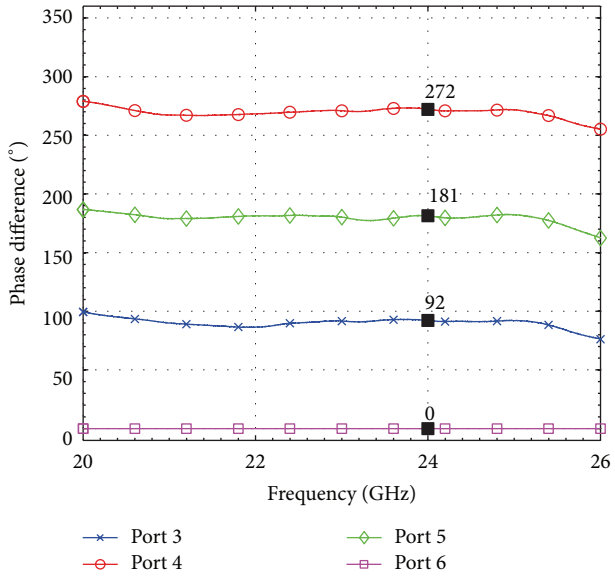

Figure 15: Measured normalized phase difference at the output ports of the Six-port network (reference port 6 is set to 0°).

7.2. Six-Port Network. Measurement results in Figure 15 and Table 1 show that the four quadrature phase shifts between 24 and 24.25 GHz can be obtained with only 2° deviation, which is due to the optimal phase shift performance of the quadrature hybrid coupler.

Moreover, the designed Six-port network features high isolation between input ports 1 and 2 (−30 dB). The return loss at the input ports is lower than −15 dB, while at the output ports 3, 4, 5, and 6 it is lower than −20 dB. Furthermore, the power imbalance at the output ports is less than 1.7 dB, as shown in Figures 16 and 17.

7.3. Theoretical Distance Accuracy Limits. A circuit simulation with Agilent Advanced Design System has been performed in order to estimate the theoretical accuracy of the radar front-end due to the imperfections of the Six-port network and the quadrature hybrid coupler used as radar coupler. The measured *S*-parameters of the coupler result in a maximum phase shift error $\Delta\sigma_{\text{err}} = \pm 11.5^\circ$ and therefore in a maximum distance measurement error $d_{\text{err}} = \pm 200\,\mu$m. System simulation with the measured Six-port network performance and apart from that an ideal RF front-end results in $\Delta\sigma_{\text{err}} = \pm 7.5^\circ$ and $d_{\text{err}} = \pm 130\,\mu$m. Using the measured *S*-parameters of Six-port network and coupler leads to a maximum phase shift error $\Delta\sigma_{\text{err}} = \pm 12^\circ$ and a maximum error of the measured distance $d_{\text{err}} = \pm 210\,\mu$m.

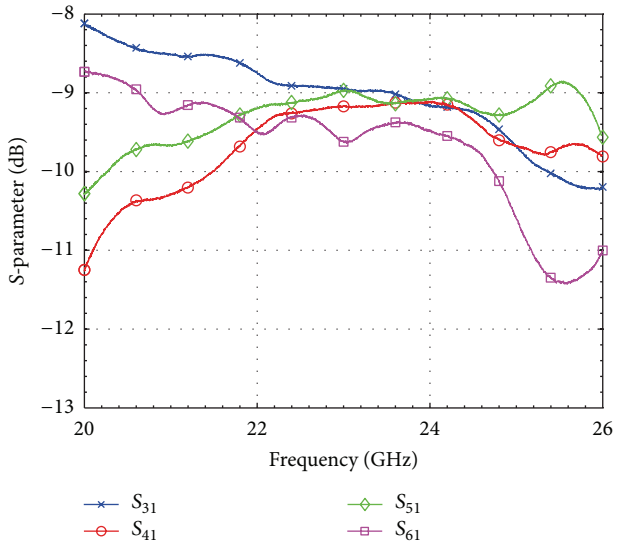

Figure 16: Six-port: measured transmission from port 1 to the output ports.

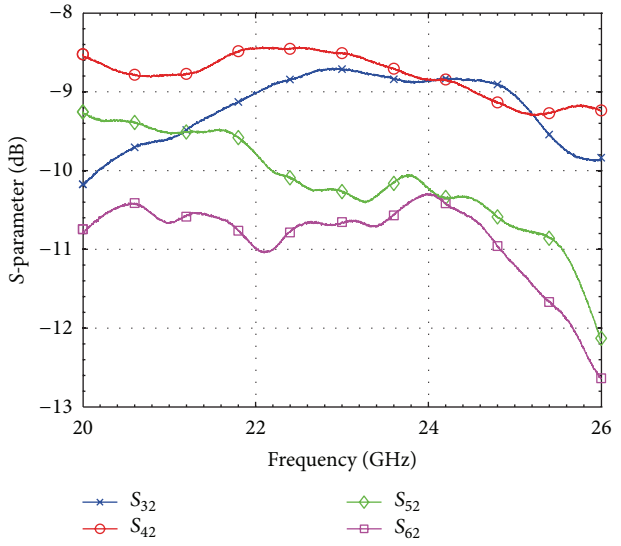

Figure 17: Six-port: measured transmission from port 2 to the output ports.

These measurement errors have a characteristic sinusoidal shape. Consequently, they can be compensated by a suitable calibration. The same holds for measurement errors due to additional static targets, for example, in an industrial environment. These have a periodicity of $\lambda/4$ and can be compensated.

7.4. Distance Measurements. The Six-port radar system has been tested by sweeping the position of a corner reflector used as a target with the help of a high precision computer controlled linear stage. The target has been placed at a distance of 1.7 m and shifted by 150 mm towards the radar with steps of 100 μm. The reference for the positioning system

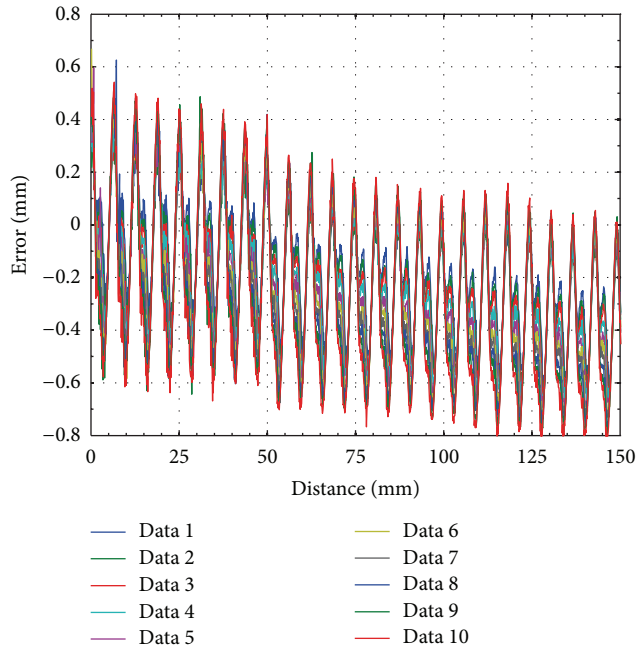

Figure 18: Absolute measurement error.

is the optical encoder of the linear stage which features a resolution of 0.5 μm. The measurement has been repeated ten times in one hour time frame. The target's displacement has been calculated from the measured phase with (5).

In order to get a more detailed view of the results, the absolute measurement error has been calculated and is shown in Figure 18 for all datasets. A constant drift of the offset and a similar periodic behavior of all datasets can be observed. Nevertheless, this error can be compensated as it is equal for all measurements and therefore, characteristic for the system. For this reason, after a calibration based on one dataset, the relative error has been calculated and is presented in Figure 19. The variation of the relative error between minimum and maximum is due to a constant and slow drift between the datasets and is probably caused by a system's temperature change within the measurement time frame of one hour.

In order to evaluate the system's accuracy independently from this constant drift over time, 10,000 measurement values have been recorded with an interval of 10 ms resulting in a total measurement time frame of 100 s. The standard deviation of the measured position expressed in relative result frequency is plotted in Figure 20. 83.8% of the measured position values lies within ±20 μm around the actual position value. 99.6% lies within ±40 μm.

8. Conclusion

A compact, versatile radar module based on the Six-port technique working in the ISM band at 24 GHz has been presented. The monostatic radar system measures only (40 × 60 × 44) mm^3 and features a high integration of all

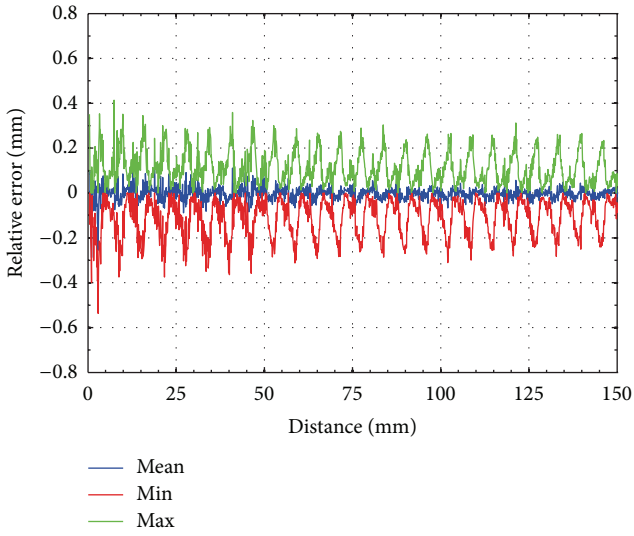

Figure 19: Relative measurement error.

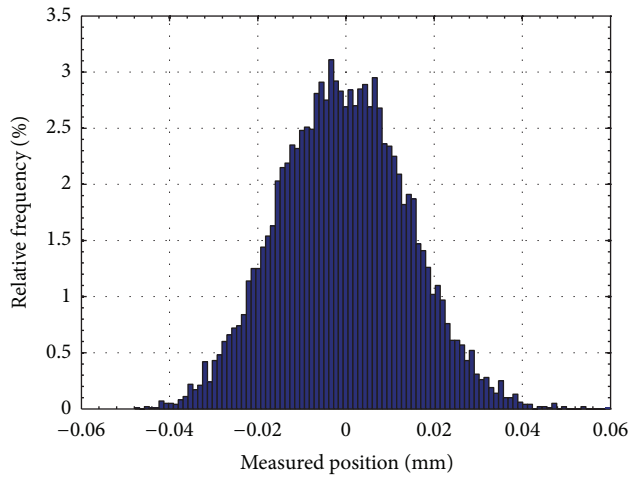

Figure 20: Standard deviation of measurement results.

subcomponents such as RF source, patch antenna array, Six-port based receiver, baseband circuitry, and digital signal processing in one single housing. Simulation results of the passive microwave components have been validated with measurements showing good design performance. An overall evaluation of the radar system demonstrates a high precision in the micrometer range (±40 μm) and a maximum relative error of ±400 μm due to a slow drift over time. These positive results are due to the excellent phase discrimination properties of the Six-port receiver. The proposed system is therefore suitable for several industrial and medical applications where high measurement accuracy is required such as displacement and vibration measurements as well as remote breath and heartbeat monitoring.

Acknowledgments

The authors would like to thank Holger Ebert, Thomas Popp, and other engineers from the R&D department, Industrial Division at InnoSenT GmbH for the technical support and for the production of the sensors modules in the company's manufacturing facilities.

References

[1] F. Barbon, G. Vinci, S. Lindner, R. Weigel, and A. Koelpin, "A six-port interferometer based micrometer-accuracy displacement and vibration measurement radar," in *Proceedings of the IEEE MTT-S International Microwave Symposium Digest (MTT '12)*, pp. 1–3, 2012.

[2] G. Vinci, S. Lindner, S. Mann et al., "Six-port microwave interferometer radar for mechanical vibration analysis," in *Proceedings of the European Radar Conference*, Nuremberg, Germany, 2013.

[3] A. Stelzer, "A microwave position sensor with submillimeter accuracy," *IEEE Transactions on Microwave Theory and Techniques*, vol. 47, no. 12, pp. 2621–2624, 1999.

[4] S. Ayhan, M. Pauli, T. Kayser, S. Scherr, and T. Zwick, "FMCW radar system with additional phase evaluation for high accuracy range detection," in *Proceedings of the 8th European Radar Conference (EuRAD '11)*, pp. 117–120, October 2011.

[5] G. Vinci, S. Lindner, F. Barbon et al., "24 GHz six-port medical radar for contactless respiration detection and heartbeat monitoring," in *Proceedings of the 9th European Radar Conference (EuRAD '12)*, pp. 75–78, 2012.

[6] A. Koelpin, G. Vinci, B. Laemmle, S. Lindner, F. Barbon, and R. Weigel, "Six-port technology for traffic safety," *IEEE Microwave Magazine*, vol. 13, no. 3, pp. 118–127, 2012.

[7] G. Vinci, F. Barbon, B. Laemmle, R. Weigel, and A. Koelpin, "A widerange 77 GHz Direction of Arrival detector with integrated dual six-port receiver," in *Proceedings of the International Microwave Symposium (IMS '12)*, Montreal, Canada, 2012.

[8] C. A. Hoer, "Using six-port and eight-port junctions to measure active and passive circuit parameters," NBS Tech. Note 673, 1975.

[9] G. F. Engen, "The six-port reflectometer: an alternative network analyzer," *IEEE Transactions on Microwave Theory and Techniques*, vol. 25, no. 12, pp. 1075–1080, 1977.

[10] F. M. Ghannouchi and A. Mohammadi, *The Six-Port Technique with Microwave and Wireless Applications*, Artech House, 2009.

[11] G. Vinci, S. Lindner, F. Barbon et al., "Six-port radar sensor for remote respiration rate and heartbeat vital-sign monitoring," *IEEE Transactions on Microwave Theory and Techniques*, vol. 61, no. 5, pp. 2093–2100, 2013.

[12] A. Koelpin, G. Vinci, F. Barbon, S. Lindner, R. Weigel, and G. Fischer, "The six-port technology: a low-cost concept for precise position measurements," in *Proceedings of the International Multi-Conference on Systems, Signals and Devices (SSD '12)*, Chemnitz, Germany, 2012.

[13] M. Jahn, C. Wagner, and A. Stelzer, "DC-offset compensation concept for monostatic FMCW radar transceivers," *IEEE Microwave and Wireless Components Letters*, vol. 20, no. 9, pp. 525–527, 2010.

[14] A. Koelpin, G. Vinci, B. Laemmle, D. Kissinger, and R. Weigel, "The six-port in modern society," *IEEE Microwave Magazine*, vol. 11, no. 7, pp. S35–S43, 2010.

[15] S. Lindner, G. Vinci, F. Barbon, S. Mann, R. Weigel, and A. Koelpin, "Dual tone approach for unambiguous six-port based interferometric distance measurements," in *Proceedings of the International Microwave Symposium (IMS '13)*, Seattle, Wash, USA, 2013.

[16] B. Bonkari, E. Moldovan, S. Affes, K. Wu, R. G. Bosisio, and S. O. Tatu, "Six-port FMCW collision avoidance radar sensor configurations," in *Proceedings of the IEEE Canadian Conference on Electrical and Computer Engineering (CCECE '08)*, pp. 305–308, May 2008.

[17] D. M. Pozar, *Microwave Engineering*, John Wiley and Sons, 2005.

[18] P. Pahl, T. Kayser, M. Pauli, and T. Zwick, "Evaluation of a high accuracy range detection algorithm for FMCW/Phase radar systems," in *Proceedings of the 7th European Radar Conference (EuRAD '10)*, pp. 160–163, October 2010.